Journal of Advanced Research in Natural and Applied Sciences
dergipark.org.tr/en/pub/jarnas
Open Access

ISSN: 2757-5195 11 (1) (2025) 63-71 doi.org/10.28979/jarnas.1627038

Microstructure and Mechanical Behavior of $CaCO_3$-Doped Al–Al_2O_3 Composite Foams Produced by Powder Metallurgy

Nebi Demirbağ[1], Serkan Abalı[2]

Article Info
Received: 25 Jan 2025
Accepted: 27 Feb 2025
Published: 31 Mar 2025
Research Article

Abstract − In this study, closed-cell composite metal foam production was performed using the powder metallurgy method. Therefore, 7, 12, and 17 wt.% $CaCO_3$ as a foaming agent was added to the Al–Al_2O_3 powder mixture containing 5 wt.% Al_2O_3 after the grinding process. The $CaCO_3$-added Al–Al_2O_3 powder mixture was mixed wet and pulverized in a mortar after drying in an oven. Three separate powder mixtures were formed under a pressure of 40 MPa and sintered at 550 °C for 1 h and then at 1000 °C for 4 h. The samples' densities, mineralogical properties, microstructures, adsorption isotherms, and compressive strengths were investigated after sintering. The effects of different $CaCO_3$ ratios on the mechanical and microstructural properties of the composite metal foam were investigated under specific production conditions. The foam material produced from the mixture with 7 wt.% $CaCO_3$ added by weight had the highest compressive strength and a more homogeneous pore distribution.

Keywords − *Ceramic, metal, composite, foam, powder metallurgy*

1. Introduction

Closed-cell aluminum metal foams have a wide research area because of their mechanical strength and impact absorption capacity, such as high compression, bending strength, and damping. [1–4]. In particular, Al alloy closed-cell metal foams are used in automotive and aviation industries [5]. The inner surfaces cannot be reached in closed-cell metal foams because of the isolated pores. The powder metallurgy method is generally used to produce open-cell metal foams [6]. However, studies have also been using the powder metallurgy method to produce closed-cell metal foams [7–9]. Unlike the melting method, sintering with powder metallurgy can prevent the sudden melting of the metal alloy before the release of gas from the foamer. If gas release ends before the metal melts, the melted metal cannot be transferred. The powder metallurgy method has been observed to work even when the metal alloy is in a solid state. The powder metallurgy technique also reduces the gas release temperature of the foamer compared with the metal melting method [10, 11]. $CaCO_3$, as a foaming agent, is easily available, and its wettability of the Al melt is as good as that of the conventional foaming agent TiH_2 [12]. The metal alloy should not melt before $CaCO_3$ is wholly calcined. That is, homogeneity can be achieved before most of the gas is released [9]. Therefore, reinforcement can be made with a suitable additive material to increase the melting point of Al metal.

[1]nebidemirbag@gmail.com; [2]sabali@comu.edu.tr (Corresponding Author)
[1]Department of Bioengineering and Materials Engineering, School of Graduate Studies, Çanakkale Onsekiz Mart University, Çanakkale, Türkiye
[2]Department of Materials Science and Engineering, Faculty of Engineering, Çanakkale Onsekiz Mart University, Çanakkale, Türkiye

One such reinforcement is Al_2O_3. Al_2O_3 also provides strength to the metal foams [13]. Lightness increases as the porosity increases in metal foams, but the mechanical properties decrease, and impact absorption properties are negatively affected [14]. However, it is possible to increase both the porosity and mechanical properties [15]. For this reason, reinforcing Al metal foam with Al_2O_3 ceramic and using powder metallurgy techniques can effectively preserve the mechanical strength without reducing the porosity. The biggest problem in metal foam production is the lack of control over process parameters [16]. The powder metallurgy method also allows control of these parameters [17]. In the production of metal foam by the melting method, it is difficult to control the pressure during cooling after mixing the foaming agent into a molten alloy. Thus, deformation often occurs in products. There is no handicap in the powder metallurgy method. In the powder metallurgy method, it is easy to control the pore size distribution and morphology by adding a foaming agent, which is one of the process parameters [18]. Particle sintering via powder metallurgy increases the expansion of the foam, resulting in a more homogeneous porosity and microstructure. [19].

In this study, we aimed to determine and compare the properties of materials with sufficient porosity and strength using different amounts of foaming agents in producing Al-based Al–Al_2O_3 metal composite foams. In the initial composition, where the amount of ceramic material remained constant, the specific changes in the metal/ceramic foam filter were measured as Al increased and the foaming agent decreased or vice versa. The effect of the increase or decrease in Al on the gas release during powder metallurgy can be understood as a result of the characterization tests.

2. Materials and Methods

The raw materials used in the study were commercially available Al powders (≤ 100 μm), Al_2O_3 powders (≤ 100 μm), and $CaCO_3$ powders (≤ 500 μm). In this study, Al–Al_2O_3 metal foams were produced using the powder metallurgy method. $CaCO_3$ was used as a foaming agent. The initial compositions of the samples are listed in Table 1. Each sample was coded in a table according to its percentage ratio. AA7C, AA12C, and AA17C refer to Al–Al_2O_3 powder mixture with 7%, 12%, and 17% $CaCO_3$ by weight, respectively.

Table 1. Compositions of samples for raw material preparation

Sample code	Raw material (wt.%)		
	Aluminum	Alumina	Calcite
AA7C	88	5	7
AA12C	83	5	12
AA17C	78	5	17

Each raw material was weighed on an analytical balance (Shimadzu, Unibloc AUX 320, Kyoto, Japan) according to the composition values, and the samples were ground for homogeneous mixing (Restch RS 200, Haan, Germany). Then, the samples were mixed on a magnetic stirrer (IKA C-MAG HS7, Staufen, Germany), and after being dispersed in a mortar, they were dried at 100°C in a vacuum oven (Nüve EV 018, Ankara, Türkiye). Three separate powder mixtures (Nannenti Mignon S, Faenza, Italy) were pressed at 40 MPa, and two-stage sintering was performed to ensure a porous and durable material formation. In the first stage, sintering was performed for 1 h in air at 550 °C, and in the second stage, sintering was performed for 4 h in air at 1000 °C (Protherm PLF 110/8, Ankara, Türkiye) to obtain the disc-shaped semi-finished products.

Compressive tests were performed on a universal testing machine (Shimadzu AG-XD, Kyoto, Japan) at a 5 mm/min speed, according to ASTM E9-89a. The specimens had a diameter of 57 mm and a length of 7 mm. The pore volumes of the samples were measured using a Brunauer–Emmett–Teller surface area analyzer (Micromeritics Gemini VII, USA). Nitrogen adsorption measurements were performed for all the samples after degassing for 3 h at 300 °C. Mineralogical analyses of the samples were performed using X-ray diffraction

(XRD, PANalytical Empyrean). The phase quantities of the samples sintered at different temperatures were obtained using the PANalytical HighScore Plus software based on the Rietveld method. The samples were scanned using Cu Kα radiation in the 2θ range of 10–80°. Scanning electron microscopy (ZEISS Gemini SEM 500-71-08) was used to evaluate the porosity and morphological changes in the internal structure as a function of the sample composition. The density of each foam was determined based on Archimedes' principle according to the ASTM D 792 standard test method (Metler, Switzerland).

3. Results and Discussion

The maximum compressive strengths of the samples were better than those in the study conducted by Alizadeh and Aliabadi [20] with Al–Al_2O_3 composite metal foams. Similar results were obtained for the compressive strengths of Al metal foams using $CaCO_3$ as a foaming agent by Aboraia et al. [21]. As shown in the compressive stress-displacement diagram in Figure 1, the foam sample obtained from the raw material mixture containing 7 wt. % $CaCO_3$ had a lower strain rate at the same stress than the other two samples. The maximum stresses and percentage elongations of samples AA7C, AA12C and AA17C are 23.10 MPa (22.24%), 22.67 MPa (32.72%) and 23.12 MPa (29.55%), respectively. In addition, the AA7C sample had a higher stress for the same strain rate. When the $CaCO_3$ ratio increased, the compressive strength decreased at the same strain rate (AA12C), and when it was increased further (AA17C), it increased but remained below the compressive strength of AA7C. Although the strengths of the AA12C and AA17C samples were similar, that of AA7C was different. Therefore, it is beneficial for the $CaCO_3$ ratio not to exceed the limit of 7% by weight in terms of compressive strength. In addition, the $CaCO_3$ ratio is 7% by weight compared to the other samples means that the Al ratio is high, and not only the low porosity but also the high Al content is effective at high strength. Higher Al in the initial composition may provide strength, but it may also have caused a mechanism that will delay the completion of melting and provide gas release. In this case, the use of 7 wt. % foaming agent provided the best result in terms of compressive strength. Increasing the foaming agent ratio (> 7% by weight) increased the porosity ratio, causing the final structure to collapse into the cell walls under tension, causing deformation and losing strength [22].

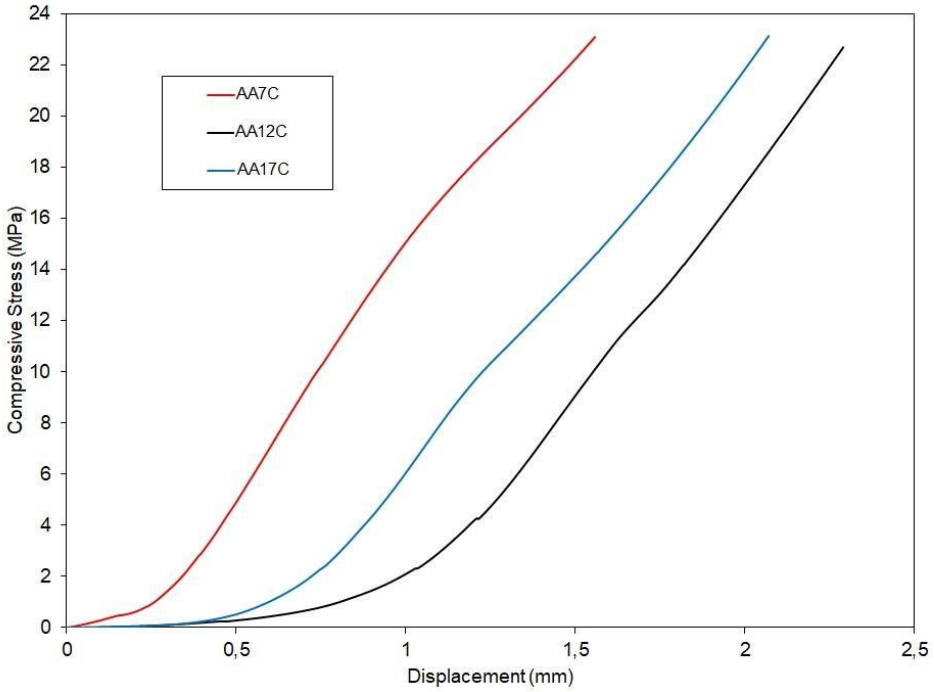

Figure 1. Compressive stress–displacement curves of the samples

Figure 2 shows the nitrogen adsorption isotherms of the samples. According to the IUPAC classification, the adsorption isotherms are type III isotherms [23]. The system does not show significant macro and mesopore formation. At high relative pressure ($0.9<P/P_0$), there are distinct hysteresis loops in the samples (AA7C, AA17C) containing high and low $CaCO_3$. In the AA12C sample, sufficient adsorption could not occur at high pressures. The fact that the adsorption pressure occurs at high volumes, although not at a high rate, shows that adsorption occurs in macropores. It is known that foams containing macropores have sufficient mechanical strength [24]. Although macropores are low, the highest adsorption volume is in the AA7C sample with 28.56 cm^3g^{-1} as shown in the isotherm curves. This is also consistent with the compression test that resulted from the high Al and low $CaCO_3$ in the initial composition. Although they have similar adsorption volumes, AA17C sample has higher volume ratios (up to 12.28 cm^3g^{-1}) than AA7C sample at high pressures. Thus, it shows that the porosity of AA17C sample is high, although not much difference. This difference is consistent with the compressive strength in Figure 1. The lower porosity of AA7C sample causes it to be slightly more durable. In addition, although the porosity of AA7C sample is lower than AA17C sample, it is shown that there is not much difference between them in terms of isotherm curves. Thus, a durable Al–Al_2O_3 metal-based foam can be obtained without reducing the porosity too much. The fact that there is a less curved cycle in the isotherm curve of AA7C sample at high pressure ($0.9<P/P_0$) compared to AA17C sample indicates that the pore distribution of AA7C sample is homogeneous, and there are similar-sized pores.

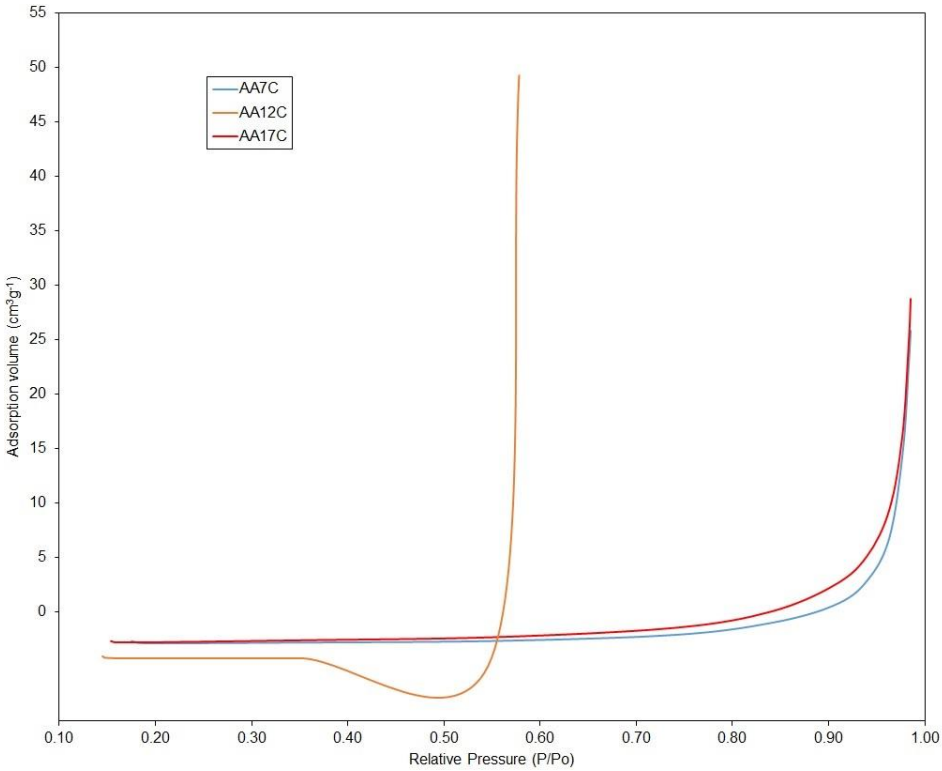

Figure 2. Nitrogen adsorption isotherm curves of samples containing $CaCO_3$ and Al in different ratios

The quantitative analysis results of the metal-ceramic foams prepared with different proportions of the foaming agent are shown in Table 2. In the AA7C sample, which is rich in Al compared to the other samples in the initial composition, Al is converted to corundum at a higher rate than in the different samples. This result also explains the reason for the highest compressive strength in the stress-strain curve shown in Figure 1. In addition, the AA7C sample had the lowest porosity according to the adsorption isotherms. The high level of corundum and low porosity compared with the other samples result from the high compressive strength. The presence of corundum indicates that the crystallization is complete, sufficient time is provided for gas release, and the sudden melting of Al in the initial composition eliminates the negativity. The high melting temperature of corundum delayed the complete melting of Al in the matrix, providing sufficient time for gas release. Thus, controllable conditions were provided for optimum metal/ceramic foam production.

Table 2. Quantitative analysis of Al–Al_2O_3 foams prepared with different foaming ratios

Sample code	Phase composition (wt.%)				
	Corundum	Aluminum	Portlandite	Grossite	Calcite
AA7C	50.4	41.9	2.2	4.7	0.8
AA12C	42.0	56.7	-	1.2	0.1
AA17C	42.4	50.9	1.1	5.2	0.4

As shown by the Al peak intensities in Figure 3, the Al ratio in the AA7C sample decreased compared to that in the AA12C and AA17C samples. More Al and less $CaCO_3$ in the initial composition resulted in a greater corundum transformation. The reactions that occurred due to the increase in the foaming agent ratio must have decreased the amount of corundum. In the Al–Al_2O_3/$CaCO_3$ system, Al is oxidized and transformed into corundum at high temperatures. As the temperature increased, Al was oxidized, and more corundum was formed. During this time, CaO formed by the decomposition of $CaCO_3$ reacts with Al_2O_3 in the system to form $CaAl_2O_4$ [25]. However, in our study, although the temperature was kept constant, more Al in the initial composition of the AA7C sample acted as a catalyst, allowing more corundum to emerge, as shown by the mineralogical analysis results. However, less $CaCO_3$ in the initial composition of the AA7C sample indicates that CaO reacts with less Al_2O_3 than the other samples, which is another factor explaining why corundum is more abundant in the AA7C sample. In other words, corundum formation can be provided with sufficient porosity to increase the mechanical strength without increasing temperature.

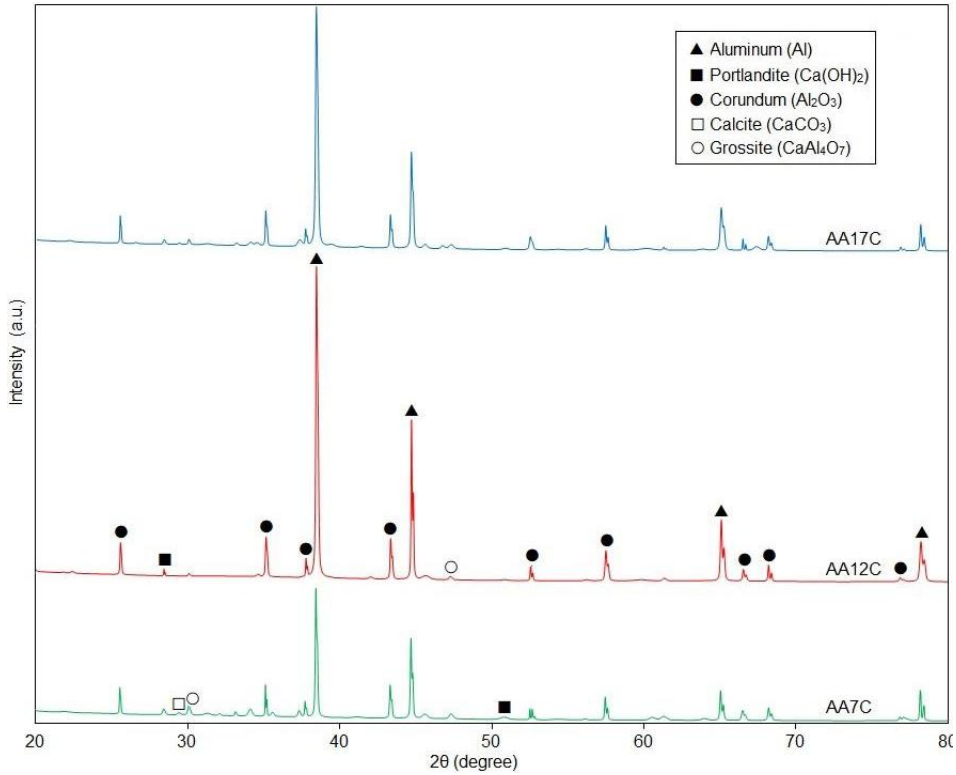

Figure 3. X-ray diffraction (XRD) patterns of the samples

When the AA7C and AA12C samples were compared, increasing the amount of $CaCO_3$ foaming agent used from 7% to 12% by weight slightly increased the porosity. However, acceptable porosity and high strength required for a foam material were formed in the AA7C sample. However, the fact that Al was lower in the AA7C sample in the mineralogical analysis may create a disadvantage regarding material ductility. However, the difference between the Al contents of the two samples was not as high as the difference between the

strength values. Therefore, the AA7C sample could be evaluated on an industrial scale in terms of both the best strength and acceptable porosity rates.

Figure 4 shows the microstructure images of all the samples. When the SEM images of the AA7C and AA17C samples were examined, it was found that the pores were concentrated in certain regions in the AA17C sample. At the same time, they tended to show a more homogeneous distribution in the AA7C sample.

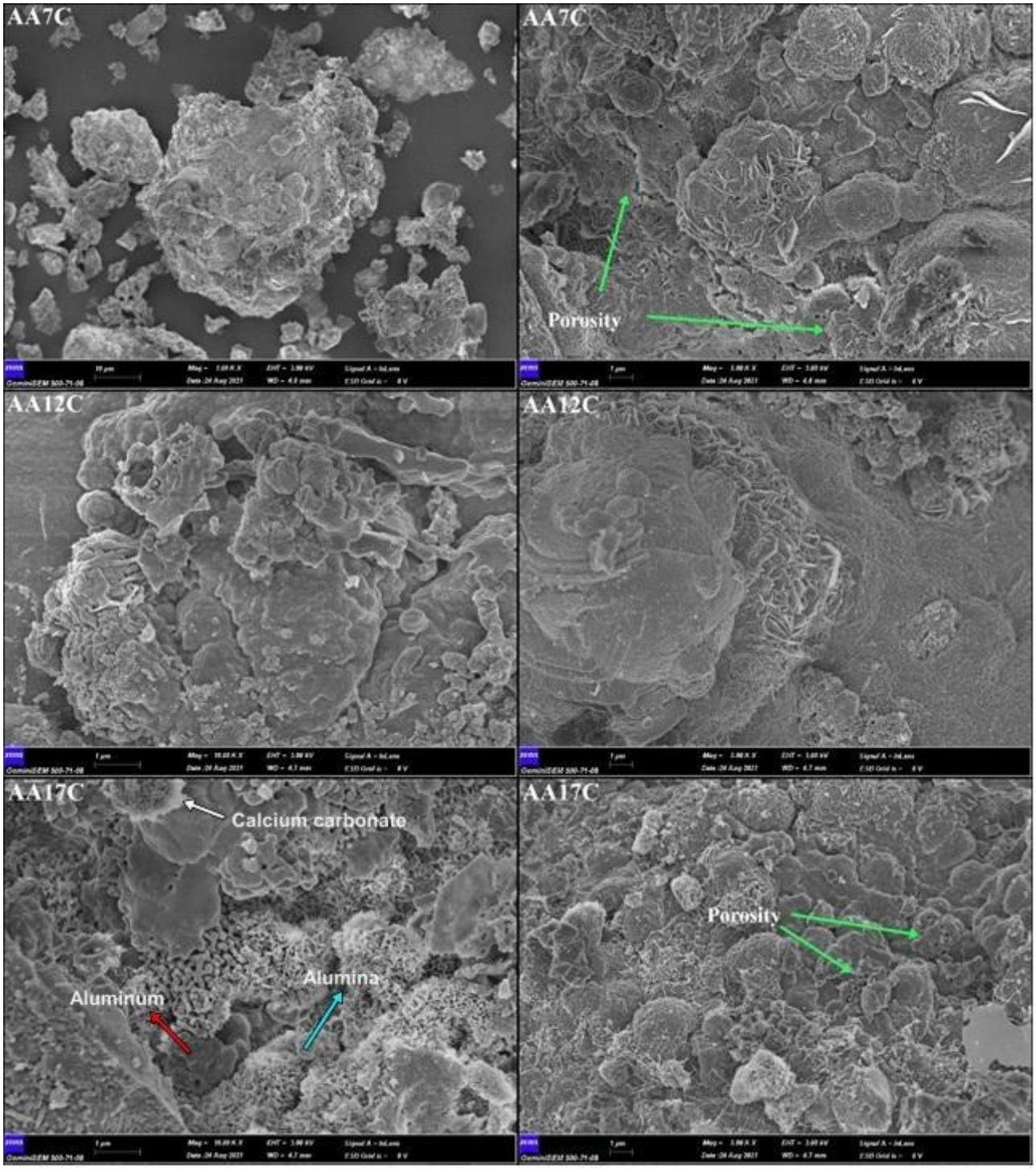

Figure 4. SEM images of Al–Al_2O_3 metal-ceramic samples using 7% (AA7C), 12% (AA12C) and 17% (AA17C) $CaCO_3$ by weight as foaming agent

The homogeneous distribution of pores can positively affect the strength of the AA7C sample. The quantitatively high corundum, partially fewer pores, and homogeneous pore distribution explain why the AA7C sample has a higher strength than the AA17C sample. When the microstructure of the AA12C sample

was examined, almost non-existent pores explained why the sample could not show adsorption in the isotherm curves. Although the initial composition of $CaCO_3$ in the AA12C sample has an intermediate rate compared with the other samples, it is understood that the $CaCO_3$ to CaO transformation is not complete. The incomplete gas evolution in the AA12C sample is explained by the high peak intensity of Al in the mineralogical analysis, as shown in Figure 3. This is because reactions that provide sufficient pores do not occur. However, Al was more abundant in the initial AA12C composition. SEM analyses indicated dark grey as the Al phase, light grey as the Al_2O_3 phase, and white as the $CaCO_3$ phase. The images show that the Al_2O_3 phase is denser in the AA7C sample, and the $CaCO_3$ phase is denser in the AA17C sample. The Al phase was the matrix phase in all samples.

Table 3 shows the experimental density results of Al–Al_2O_3 materials containing different weight ratios of foaming agent and Al. Although there is no obvious density difference between the three samples, the density of the AA7C sample is higher. This result is also consistent with the compressive strength. However, the density in the AA7C sample is not at a level that will have a negative effect on the porosity of the Al–Al_2O_3 material. It is not desired for the foams to have a very low density in terms of strength. In addition, the foams are expected to provide sufficient vitrification and crystallization during production, which is unsuitable for very low density. Therefore, although the AA7C sample is higher, all samples have acceptable densities for metal foams [15].

Table 3. Densities of samples at different initial compositions

Sample	Density (gr/cm^3)
AA7C	2.71
AA12C	2.65
AA17C	2.63

4. Conclusion

Using the powder metallurgy method, closed-pore metal-based foam production can be achieved with ceramic additives and sufficient foaming agents. The AA7C sample provides sufficient properties for the production of metal-based ceramic-added foams with a high corundum phase formed as a result of crystallization, a 23.10 MPa compressive strength with a small displacement of 1.5 mm, sufficient density, low macroporous content, high adsorption volume at high pressure, and homogeneous pore distribution, especially without the need for an increase in temperature. It was revealed that the closed pore structure of the foam does not create any obstacles in gas release without melting. In addition, the low $CaCO_3$ ratio in the Al–Al_2O_3 structures causes CaO to react with less Al_2O_3 and acts as a catalyst to convert more Al into Al_2O_3.

Author Contributions

This paper is derived from the first author's master's thesis supervised by the second author. The first author proposed the study and wrote the manuscript. The second author designed and performed the experiments. They all read and approved the final version of the paper.

Conflict of Interest

All the authors declare no conflict of interest.

Ethical Review and Approval

No approval from the Board of Ethics is required.

Acknowledgment

The authors thank Dr. Emin Yakar for his essential support in conducting the analysis for this study.

References

[1] S. U. Nisa, S. Pandey, P. Pandey, *A review of the compressive properties of closed-cell aluminum metal foams*, Proceedings of the Institution of Mechanical Engineers, Part E: Journal of Process Mechanical Engineering 237 (2) (2022) 531–545.

[2] M. I. Idris, T. Vodenitcharova, M. Hoffman, *Mechanical behaviour and energy absorption of closed-cell aluminium foam panels in uniaxial compression*, Materials Science and Engineering: A 517 (1-2) (2009) 37–45.

[3] Y. J. Yang, F. S. Han, D. K. Yang, K. Zheng, *Compressive behaviour of open cell Al–Al_2O_3 composite foams fabricated by sintering and Dissolution Process*, Materials Science and Technology 23 (4) (2007) 502–504.

[4] C. Betts, *Benefits of metal foams and developments in modelling techniques to assess their materials behaviour: A review*, Materials Science and Technology 28 (2) (2012) 129–143.

[5] I. Duarte, J. Ferreira, *Composite and nanocomposite metal foams*, Materials 9 (2) (2016) 79.

[6] M. Madgule, C. G. Sreenivasa, A. V. Borgaonkar, *Aluminium metal foam production methods, properties and applications- A review*, Materials Today: Proceedings 77 (2023) 673–679.

[7] B. P. Neville, A. Rabiei, *Composite metal foams processed through powder metallurgy*, Materials and Design 29 (2) (2008) 388–396.

[8] B. Han, Y. Li, Z. Wang, X. Gu, Q. Zhang, *Temperature effects on the compressive behaviors of closed-cell copper foams prepared by powder metallurgy*, Materials 14 (21) (2021) 6405.

[9] D. Yang, Z. Hu, W. Chen, J. Lu, J. Chen, H. Wang, L. Wang, J. Jiang, A. Ma, *Fabrication of Mg-Al alloy foam with close-cell structure by powder metallurgy approach and its mechanical properties*, Journal of Manufacturing Processes 22 (2016) 290–296.

[10] V. Kevorkijan, *Low cost aluminium foams made by $CaCO_3$ particulates*, Association of Metallurgical Engineers of Serbia 16 (3) (2010) 205–219.

[11] N. Behymer, K. Morsi, *Review: Closed-cell metallic foams produced via powder metallurgy*, Metals 13 (5) (2023) 959.

[12] T. Nakamura, S. Gnyloskurenko, K. Sakamoto, A. Byakova, R. Ishikawa, *Development of new foaming agent for metal foam*, Materials Transactions 43 (5) (2002) 1191–1196.

[13] M. Alizadeh, M. Mirzaei-Aliabadi, *Compressive properties and energy absorption behavior of Al–Al_2O_3 composite foam synthesized by space-holder technique*, Materials and Design 35 (2012) 419–424.

[14] H. Nakajima, *Fabrication, properties and application of porous metals with directional pores*, Progress in Materials Science 52 (7) (2007) 1091–1173.

[15] C. S. Jee, Z.X. Guo, J. R. Evans, N. Özgüven, *Preparation of high porosity metal foams*, Metallurgical and Materials Transactions B 31 (2000) 1345–1352.

[16] B. Bauer, S. Kralj, M. Busic, *Production and application of metal foams in casting technology*, Tehnicki Vjesnik-Technical Gazette 20 (6) (2013) 1095–1102.

[17] S. Singh, N. Bhatnagar, *A survey of fabrication and application of metallic foams (1925–2017)*, Journal of Porous Materials 25 (2018) 537–554.

[18] U. Waag, L. Sclmeider. *Metallic hollow spheres—materials for the future*, Metal Powder Report 55 (1) (2000) 29–33.

[19] A.M. Medina Ramirez, R.R. Vintila, R.A. Drew, *Morphology of aluminum alloy foams produced with dolomite via partial sintering of precursors*, Materials 12 (10) (2019) 1691.

[20] M. Alizadeh, M. Mirzaei-Aliabadi, *Compressive properties and energy absorption behavior of Al–Al_2O_3 composite foam synthesized by space-holder technique*, Materials and Design 35 (2012) 419–424.

[21] M. Aboraia, R. Sharkawi, M.A. Doheim, *Production of aluminium foam and the effect of calcium carbonate as a foaming agent*, Journal of Engineering Sciences 39 (2) (2011) 441–451.

[22] S.U. Nisa, S. Pandey, P. Pandey, *A review of the compressive properties of closed-cell aluminum metal foams*, Proceedings of the Institution of Mechanical Engineers, Part E: Journal of Process Mechanical Engineering 237 (2) (2022) 531–545.

[23] K. S. Sing, *Reporting physisorption data for gas/solid systems with special reference to the determination of surface area and porosity (recommendations 1984)*, Pure and Applied Chemistry 57 (4) (1985) 603–619.

[24] N. Kota, M. S. Charan, T. Laha, S. Roy, *Review on development of metal/ceramic interpenetrating phase composites and critical analysis of their properties*, Ceramics International 48 (2) (2022) 1451–1483.

[25] K. Córdova-Szymanski, E. Armendaríz-Mireles, J. Rodríguez-García, J. Miranda-Hernández, E. Rocha-Rangel, *Production of cement based on calcium aluminate by means of solid-state reactions*, Chemistry and Chemical Technology 16 (3) (2022) 492–498.